JCAMECH

Vol. 51, No. 1, June 2020, pp 231-238
DOI: 10.22059/jcamech.2019.272602.351

Analytical buckling and post-buckling characteristics of Mindlin micro composite plate with central opening by use of nonlocal elasticity theory

*Majid Jamali, Taghi Shojaee, Bijan Mohammadi**

School of Mechanical Engineering, Iran University of Science and Technology, Tehran, Iran

ARTICLE INFO

ABSTRACT

Article history:
Received: 30 December 2018
Accepted: 1 April 2019

Keywords:
Buckling and nonlinear Post-buckling analysis
micro composite plate
Central opening; Elastic medium
Mindlin plate theory

The effect of central opening on the buckling and nonlinear post-buckling response of carbon nanotubes (CNTs) reinforced micro composite plate embedded in elastic medium is considered in this paper. It is assumed that the system is surrounded by elastic medium, therefore; the influence of Pasternak foundation on buckling and post-buckling behavior are analyzed. In order to derive the basic formulations of plate the Mindlin plate theory is applied. Furthermore, nonlocal elasticity theory is applied to consider the size-dependent effect. Analytical approach and Newton-Raphson iterative technique are utilized to calculate the impact of cut out on the buckling and nonlinear post-buckling response of micro composite plate. The variation of buckling and post-buckling of micro composite cut out plate based on some significant parameters such as volume fraction of CNTs, small scale parameter, aspect ratio, square cut out and elastic medium were discussed in details. According to the results, it is concluded that the aspect ratio and length of square cut out have negative effect on buckling and post-buckling response of micro composite plate. Furthermore, existence of CNTs in system causes improvement in the buckling and post-buckling behavior of plate. Meanwhile, considering elastic medium increases the buckling and post-buckling load of system.

1. Introduction

Many researchers incline to analyze the influence of composite plates reinforced with CNTs in recent years. It is due to the fact that applying CNTs in structure can improve the mechanical, electrical, thermal and other chemical/physical characteristics [1, 2]. Shen and Zhang [3] studied thermal buckling and post-buckling behavior of composite plates. The results demonstrate that the thermal post-buckling strength of the plate can be improved as a result of a functionally graded reinforcement. Mechanical buckling of nanocomposite rectangular plate reinforced by aligned and straight single-walled carbon nanotubes was presented by Jafari Mehrabadi et al. [4]. In this paper, the Eshelby–Mori–Tanaka approach and the extended rule of mixture were applied in order to consider the effective material properties. Liew et al. [5] carried out the post-buckling of composite cylindrical panels under axial compression using a meshless. Nonlinear post-buckling and vibration response of smart two-phase nanocomposite plates with surface-bonded piezoelectric layers under a combined mechanical, thermal and electrical loading was analyzed by Rafiee et al. [6]. Jamali et al. [7] presented buckling analysis of composite nanocomposite cut out plate using domain decomposition method and orthogonal polynomials. Buckling analysis of arbitrary two-directional functionally graded Euler-Bernoulli nano-beams based on nonlocal elasticity theory was discussed by Nejad et al. [8]. Nonlocal analysis of free vibration of bi-directional functionally graded Euler-Bernoulli nano-beams was introduced by Nejad et al. [9]. Agglomeration effects on the dynamic buckling of viscoelastic microplates reinforced with CNTs using Bolotin

* Corresponding author. Email: bijan_mohammadi@iust.ac.ir

method was analyzed by Kolahchi and Cheraghbak [10]. In this research, agglomeration effects are considered based on Mori–Tanaka approach and dynamic instability region of structure is calculated based on navier and bolotin's methods. Nejad et al. [11] presented consistent couple stress theory for free vibration analysis of Euler-Bernoulli nano-beams made of arbitrary bi-directional functionally graded materials. Hadi et al. [12] considered buckling analysis of functionally graded Euler-Bernoulli nano-beams with 3D-varying properties based on consistent couple stress theory. Nejad et al. [13] presented bending analysis of bi-directional functionally graded Euler-Bernoulli nano-beams using integral form of Eringens non-local elasticity theory.

Post buckling of nanoplates have been studied by many researches so far. Farajpour et al. [14] investigated post-buckling analysis of multi-layered graphene sheets under non-uniform biaxial compression. They analyzed the effects of nonlocal parameter, buckling mode number, compression ratio and non-uniform parameter on the post-buckling behavior of multi-layered graphene sheets. The influence of surface energy on the post-buckling behavior of nanoplates was studied by Wang and Wang [15]. They showed that the influence of surface energy on the post-buckling load of the nanoplates becomes increasingly significant when the thickness of the plate decreases. Nonlocal post-buckling behavior of both uni-axially and bi-axially loaded graphene sheets in a polymer environment according to an orthotropic nanoplate model was proposed by Naderi and Saidi [16]. Analysis of shear deformable functionally graded (FG) nanobeams in post-buckling based on modified couple stress theory was carried out by Akbarzadeh Khorshidi et al. [17]. Sahmani et al. [18] considered Size-dependent axial buckling and post-buckling characteristics of cylindrical nanoshells in different temperatures. Wu et al. [19] analyzed thermal buckling and post-buckling of FG graphene nanocomposite plates. The post-buckling response of FG nanoplates by using the nonlocal elasticity theory of Eringen to consider the size effect was studied by Thai et al. [20]. They considered the influences of gradient index, nonlocal effect, ratio of compressive loads, boundary condition, thickness ratio and aspect ratio on the post-buckling behavior of FG nanoplates.

The famous classical plate theory (CLPT) which is based on Kirchhoff's hypothesis, supposes that straight lines normal to the mid-plane will be straight and normal to the mid-plane and will not change according to thickness stretching. CLPT cannot be applied in thick plates wherein shear deformation effects are more important because the transverse shear deformation is ignored in this theory. The first order shear deformation theory (FSDT) is an improvement over the CLPT because in this theory transverse shear deformation is considered. In this theory, the transverse shear strain is presumed to be constant across the thickness; therefore, shear correction factor to correct the strain energy of shear deformation is required [21]. Ghorbanpour et al. [22] presented analytical approach for buckling analysis and smart control of a single layer graphene sheet using a coupled poly vinylidene fluoride (PVDF) nanoplate based on the nonlocal Mindlin plate theory. Buckling of FG circular/annular Mindlin nanoplates with an internal ring support using nonlocal elasticity was analyzed by Bedroud et al. [23]. Liu et al. [24] investigated the buckling and post-buckling behaviors of piezoelectric nanoplate based on the nonlocal Mindlin plate model and von Karman geometric nonlinearity. Soleimani et al. [25] attempted to investigate the nonlocal post-buckling analysis of graphene sheets with initial imperfection based on FSDT. The effect of various parameters such as nonlocal parameter, edge length, boundary conditions, compression ratio, and aspect ratio on the post-buckling was studied. The results of this work represented the high accuracy of FSDT for post-buckling behavior of graphene sheets. Size dependent free vibration analysis of nanoplates made of functionally graded materials based on nonlocal elasticity theory with high order theories was presented by Daneshmehr et al. [26].

With respect to the literature, there is not any study which is about the effect of cut out on the buckling and post-buckling behavior of micro composite plate based on Mindlin plate theory and surrounded by elastic foundation. CNTs are used to reinforce the plate through the thickness and the structure is embedded in Pasternak medium. Based on domain decomposition and Rayleigh-Ritz methods in conjunction Newton-Raphson iterative technique the post-buckling response of the system is obtained. The influence of some important parameters such as small scale effect, cut out dimension, volume fraction of CNTs, aspect ratio of plate and elastic medium on the buckling and post-buckling behavior of system are calculated.

2. Modeling of the problem

A schematic of micro composite rectangular cut out Mindlin plate with geometrical characteristics as length *a*, width *b* and thickness *h* is depicted in Figure 1. As it is obvious, the cut out shape of plate is square with length (*d*) and the system is subjected to uniaxial load (N_x). Moreover, the plate is reinforced with CNTs and the type of them through the thickness is uniform distribution (*UD*). In addition, the system resting in Pasternak foundation, which is consist of spring constant (K_w) and shear layer (G_p) for considering normal and shear loads from medium, respectively.

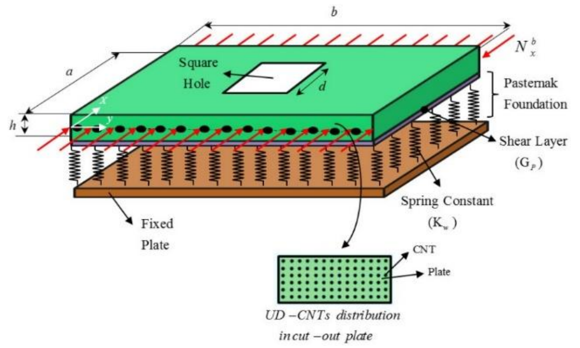

Figure 1. A schematic of a micro composite cut out plate with UD - CNTs distribution surrounded with elastic foundation subjected to uniaxial loading

2.1 Review of CNT-reinforced composite plate

The micro composite plate in this study is composed of UD-CNTs and matrix. In order to define mechanical properties of this combination, rule of mixture is employed as [27]

$$E_{11} = \eta_1 V_{CNT} E_{11}^{CNT} + V_m E^m, \tag{1}$$

$$\frac{\eta_2}{E_{22}} = \frac{V_{CNT}}{E_{22}^{CNT}} + \frac{V_m}{E^m}, \tag{2}$$

$$\frac{\eta_3}{G_{12}} = \frac{V_{CNT}}{G_{12}^{CNT}} + \frac{V_m}{G^m}, \tag{3}$$

$$V_{CNT} + V_m = 1 \tag{4}$$

in which E^m, G^m are the properties of matrix and E_{11}^{CNT}, E_{22}^{CNT} and G_{12}^{CNT} show Young's moduli and shear modulus related to CNTs, respectively. The CNTs efficiency parameter, $\eta_j\left(j=1,2,3\right)$, exposes the scale-dependent material properties defined by matching the effective mechanical properties of CNTRC. V_{CNT} and V_m demonstrate volume fractions of CNT and matrix, respectively.

In this section UD-CNTs through thickness is considered as Figure 1.

$$V_{CNT}=V_{CNT}^{*}, \qquad (UD) \tag{5}$$

in which

$$V_{CNT}^{*}=\frac{W_{CNT}}{W_{CNT}+\left(\frac{\rho_{CNT}}{\rho_m}\right)-\left(\frac{\rho_{CNT}}{\rho_m}\right)W_{CNT}}, \tag{6}$$

w_{CNT} expresses the mass fraction of nanotube, ρ_{CNT} and ρ_m define the densities of carbon nanotube and matrix, respectively. The Poisson's ratio, υ_{12} and density, ρ of micro composite plate are

$$\upsilon_{12}=V_{CNT}\upsilon_{12}^{CNT}+V_m\upsilon^m, \tag{7}$$

$$\rho=V_{CNT}\rho^{CNT}+V_m\rho^m, \tag{8}$$

where υ_{12}^{CNT} and υ^m demonstrate Poisson's ratios of CNT and matrix, respectively.

2.2 Energy analysis of nonlocal Mindlin plate theory

The displacement field based on Mindlin plate theory is explained as follows [28-30]:

$$u\left(x,y,z\right)=u_0\left(x,y\right)+z\,\phi_1\left(x,y\right), \tag{9a}$$

$$v\left(x,y,z\right)=v_0\left(x,y\right)+z\,\phi_2\left(x,y\right), \tag{9b}$$

$$w(x,y,z)=w_0(x,y), \tag{9c}$$

Where u_0, v_0 and w_0 are in-plane displacements of the mid-plane in *x*, *y* and *z* directions, respectively. ϕ_1 and ϕ_2 are the rotations about *x* and *y* directions, respectively.

According to the Eringen's nonlocal elasticity theory [31], the constitutive equations of system is related to small scale effect and atomic forces. Local and nonlocal stresses, which are defined from the nonlocal balance law, can be extracted as [32]

$$\left(1-\mu^2\nabla^2\right)\sigma_{ij}^{nl}=\sigma_{ij}^{l}=C:\varepsilon_{ij}, \quad \mu=e_0a, \tag{10}$$

where ∇^2 is the Laplace operation in the *x*-*y* coordinate system; σ_{ij}^{l} and σ_{ij}^{nl} express stress in local and nonlocal theories, respectively; *a* defines internal characteristic length, and e_0 is material constant extracted by the experiment.

Employing Eq. (10), the plane stress constitutive relation for a nonlocal FG-CNTRC micro plate is obtained as

$$\begin{Bmatrix}\sigma_{xx}^{nl}\\ \sigma_{yy}^{nl}\\ \sigma_{yz}^{nl}\\ \sigma_{xz}^{nl}\\ \sigma_{xy}^{nl}\end{Bmatrix}-\mu^2\nabla^2\begin{Bmatrix}\sigma_{xx}^{nl}\\ \sigma_{yy}^{nl}\\ \sigma_{yz}^{nl}\\ \sigma_{xz}^{nl}\\ \sigma_{xy}^{nl}\end{Bmatrix}=\begin{bmatrix}Q_{11} & Q_{12} & 0 & 0 & 0\\ & Q_{22} & 0 & 0 & 0\\ & & Q_{44} & 0 & 0\\ & & & Q_{55} & 0\\ sym. & & & & Q_{66}\end{bmatrix}\begin{Bmatrix}\varepsilon_{xx}\\ \varepsilon_{yy}\\ \gamma_{yz}\\ \gamma_{xz}\\ \gamma_{xy}\end{Bmatrix}, \tag{11}$$

$Q_{ij}\left(i,j=1,2,...,6\right)$ is defined as

$$Q_{11}=\frac{E_{11}}{1-\upsilon_{12}\upsilon_{21}}, Q_{22}=\frac{E_{22}}{1-\upsilon_{12}\upsilon_{21}}, Q_{12}=\frac{\upsilon_{21}E_{11}}{1-\upsilon_{12}\upsilon_{21}}, \\ Q_{44}=G_{23},\ Q_{55}=G_{13},\ Q_{66}=G_{12}. \tag{12}$$

The strain field extracted by applying strain-displacement relations in conjunction with von-Karman as

$$\begin{Bmatrix}\varepsilon_{xx}\\ \varepsilon_{yy}\\ \gamma_{yz}\\ \gamma_{xz}\\ \gamma_{xy}\end{Bmatrix}=\begin{Bmatrix}\varepsilon_{xx}^0\\ \varepsilon_{yy}^0\\ \gamma_{yz}^0\\ \gamma_{xz}^0\\ \gamma_{xy}^0\end{Bmatrix}+z\begin{Bmatrix}\varepsilon_{xx}^1\\ \varepsilon_{yy}^1\\ \gamma_{yz}^1\\ \gamma_{xz}^1\\ \gamma_{xy}^1\end{Bmatrix}, \tag{13}$$

in which

$$\begin{Bmatrix}\varepsilon_{xx}^0\\ \varepsilon_{yy}^0\\ \gamma_{yz}^0\\ \gamma_{xz}^0\\ \gamma_{xy}^0\end{Bmatrix}=\begin{Bmatrix}\frac{\partial u_0}{\partial x}+\frac{1}{2}\left(\frac{\partial w_0}{\partial x}\right)^2\\ \frac{\partial v_0}{\partial y}+\frac{1}{2}\left(\frac{\partial w_0}{\partial y}\right)^2\\ \frac{\partial w_0}{\partial y}+\phi_2\\ \frac{\partial w_0}{\partial x}+\phi_1\\ \frac{\partial u_0}{\partial y}+\frac{\partial v_0}{\partial x}+\frac{\partial w_0}{\partial x}\frac{\partial w_0}{\partial y}\end{Bmatrix}, \tag{14}$$

$$\begin{Bmatrix}\varepsilon_{xx}^1\\ \varepsilon_{yy}^1\\ \gamma_{yz}^1\\ \gamma_{xz}^1\\ \gamma_{xy}^1\end{Bmatrix}=\begin{Bmatrix}\frac{\partial \phi_1}{\partial x}\\ \frac{\partial \phi_2}{\partial y}\\ 0\\ 0\\ \frac{\partial \phi_1}{\partial x}+\frac{\partial \phi_2}{\partial y}\end{Bmatrix}. \tag{15}$$

The stress resultants N_{ij}^{nl}, M_{ij}^{nl} and Q_{k}^{nl} are expressed as

$$\begin{Bmatrix}N_{xx}^{nl}\\ N_{yy}^{nl}\\ N_{xy}^{nl}\end{Bmatrix}=\int_{-\frac{h}{2}}^{\frac{h}{2}}\begin{Bmatrix}\sigma_{xx}^{nl}\\ \sigma_{yy}^{nl}\\ \sigma_{xy}^{nl}\end{Bmatrix}dz, \tag{16}$$

$$\begin{Bmatrix}M_{xx}^{nl}\\ M_{yy}^{nl}\\ M_{xy}^{nl}\end{Bmatrix}=\int_{-\frac{h}{2}}^{\frac{h}{2}}z\begin{Bmatrix}\sigma_{xx}^{nl}\\ \sigma_{yy}^{nl}\\ \sigma_{xy}^{nl}\end{Bmatrix}dz, \tag{17}$$

$$\begin{Bmatrix} Q_y^{nl} \\ Q_x^{nl} \end{Bmatrix} = \kappa_s \int_{-\frac{h}{2}}^{\frac{h}{2}} \begin{Bmatrix} \sigma_{yz}^{nl} \\ \sigma_{xz}^{nl} \end{Bmatrix} dz \,, \tag{18}$$

k_s demonstrates the transverse shear correction coefficient. By using Eq. (11) with Eqs. (16-18), the nonlocal constitutive relations can be defined as

$$\begin{aligned}&\left(1-\mu^2\nabla^2\right)N_{xx}^{nl} = N_{xx} = A_{11}\frac{\partial u_0}{\partial x} + \\ &B_{11}\frac{\partial \phi_1}{\partial x} + \frac{1}{2}A_{11}\left(\frac{\partial w_0}{\partial x}\right)^2 + A_{12}\frac{\partial v_0}{\partial y} \\ &+B_{12}\frac{\partial \phi_2}{\partial y} + \frac{1}{2}A_{12}\left(\frac{\partial w_0}{\partial y}\right)^2 ,\end{aligned} \tag{19}$$

$$\begin{aligned}&\left(1-\mu^2\nabla^2\right)N_{yy}^{nl} = N_{yy} = A_{12}\frac{\partial u_0}{\partial x} + \\ &B_{12}\frac{\partial \phi_1}{\partial x} + \frac{1}{2}A_{12}\left(\frac{\partial w_0}{\partial x}\right)^2 + A_{22}\frac{\partial v_0}{\partial y} \\ &+B_{22}\frac{\partial \phi_2}{\partial y} + \frac{1}{2}A_{22}\left(\frac{\partial w_0}{\partial y}\right)^2 ,\end{aligned} \tag{20}$$

$$\begin{aligned}&\left(1-\mu^2\nabla^2\right)N_{xy}^{nl} = N_{xy} = A_{66}\frac{\partial}{\partial x}v_0 + \\ &B_{66}\frac{\partial}{\partial x}\phi_2 + A_{66}\frac{\partial}{\partial y}u_0 + B_{66}\frac{\partial}{\partial y}\phi_1 \\ &+A_{66}\left(\frac{\partial}{\partial x}w_0\right)\left(\frac{\partial}{\partial y}w_0\right),\end{aligned} \tag{21}$$

$$\begin{aligned}&\left(1-\mu^2\nabla^2\right)M_{xx}^{nl} = M_{xx} = B_{11}\frac{\partial}{\partial x}u_0 + D_{11}\frac{\partial}{\partial x}\phi_1 + \\ &0.5B_{11}\left(\frac{\partial}{\partial x}w_0\right)^2 + B_{12}\frac{\partial}{\partial y}v_0 \\ &+D_{12}\frac{\partial}{\partial y}\phi_2 + 0.5B_{12}\left(\frac{\partial}{\partial y}w_0\right)^2\end{aligned} \tag{22}$$

$$\begin{aligned}&\left(1-\mu^2\nabla^2\right)M_{yy}^{nl} = M_{yy} = B_{12}\frac{\partial}{\partial x}u_0 + D_{12}\frac{\partial}{\partial x}\phi_1 + \\ &0.5B_{12}\left(\frac{\partial}{\partial x}w_0\right)^2 + B_{22}\frac{\partial}{\partial y}v_0 \\ &+D_{22}\frac{\partial}{\partial y}\phi_2 + 0.5B_{22}\left(\frac{\partial}{\partial y}w_0\right)^2 ,\end{aligned} \tag{23}$$

$$\begin{aligned}&\left(1-\mu^2\nabla^2\right)M_{xy}^{nl} = M_{xy} = B_{66}\frac{\partial}{\partial x}v_0 + \\ &D_{66}\frac{\partial}{\partial x}\phi_2 + B_{66}\frac{\partial}{\partial y}u_0 + D_{66}\frac{\partial}{\partial y}\phi_1 \\ &+B_{66}\left(\frac{\partial}{\partial x}w_0\right)\left(\frac{\partial}{\partial y}w_0\right),\end{aligned} \tag{24}$$

$$\left(1-\mu^2\nabla^2\right)Q_{xz}^{nl} = Q_{xz} = \kappa_s A_{55}\frac{\partial}{\partial x}w_0 + \kappa_s A_{55}\phi_1 \,, \tag{25}$$

$$\left(1-\mu^2\nabla^2\right)Q_{yz}^{nl} = Q_{yz} = \kappa_s A_{44}\frac{\partial}{\partial y}w_0 + \kappa_s A_{44}\phi_2 . \tag{26}$$

the stiffness components may be extracted as

$$\left(\mathrm{A}_{ij}, \mathrm{B}_{ij}, \mathrm{D}_{ij}\right) = \int_{-\frac{h}{2}}^{\frac{h}{2}} Q_{ij}\left(z\right)\left(1, z, z^2\right)dz . \tag{27}$$

$$\begin{aligned}U &= \frac{1}{2}\int_A\int_{\frac{-h}{2}}^{\frac{h}{2}}\left(\sigma_{xx}\varepsilon_{xx} + \sigma_{yy}\varepsilon_{yy} + \sigma_{yz}\gamma_{yz} + \sigma_{xz}\gamma_{xz} + \sigma_{xy}\gamma_{xy}\right)dzdA \\ &= \frac{1}{2}\int_A\Bigg(N_{xx}\left(\frac{\partial}{\partial x}u_0 + 0.5\left(\frac{\partial}{\partial x}w_0\right)^2\right) + N_{yy}\left(\frac{\partial}{\partial y}v_0 + 0.5\left(\frac{\partial}{\partial y}w_0\right)^2\right) \\ &+ N_{xy}\left(\frac{\partial u_0}{\partial y} + \frac{\partial v_0}{\partial x} + \left(\frac{\partial w_0}{\partial x}\right)\left(\frac{\partial w_0}{\partial y}\right)\right) + M_{xx}\frac{\partial}{\partial x}\phi_1 + M_{yy}\frac{\partial}{\partial y}\phi_2 \\ &+ M_{xy}\left(\frac{\partial}{\partial y}\phi_1 + \frac{\partial}{\partial x}\phi_2\right) + Q_x\left(\frac{\partial}{\partial x}w_0 + \phi_1\right) + Q_y\left(\frac{\partial}{\partial y}w_0 + \phi_2\right)\Bigg)dA.\end{aligned} \tag{28}$$

The micro composite plate is exposed to two types of forces such as biaxial compression load and elastic medium. According to Figure 1, micro plate is subjected to uniaxial loading ($N_x^b = -F$ and $N_y^b = 0$); therefore, the work of compression load is calculated as

$$W_b = -\frac{1}{2}\int_A\left(N_x^b\left(\frac{\partial}{\partial x}w(x,y)\right)^2 + N_y^b\left(\frac{\partial}{\partial y}w(x,y)\right)^2\right)dA. \tag{29}$$

The micro plate is surrounded by elastic medium; subsequently, the work of medium is

$$W_f = -\int_A\left(K_w w - G_p\nabla^2 w\right)w\, dA , \tag{30}$$

K_w and G_p represent Winkler's spring modulus and shear foundation parameter, respectively.

Eventually, total energy of micro composite plate is defined as

$$\begin{aligned}&\Pi = U - W = \int_A\Bigg\{\frac{1}{2}\Bigg[N_{xx}\left(\frac{\partial}{\partial x}u_0 + 0.5\left(\frac{\partial}{\partial x}w_0\right)^2\right) + \\ &N_{yy}\left(\frac{\partial}{\partial y}v_0 + 0.5\left(\frac{\partial}{\partial y}w_0\right)^2\right) + N_{xy}\left(\frac{\partial u_0}{\partial y} + \frac{\partial v_0}{\partial x} + \left(\frac{\partial w_0}{\partial x}\right)\left(\frac{\partial w_0}{\partial y}\right)\right) \\ &+M_{xx}\frac{\partial}{\partial x}\phi_1 + M_{yy}\frac{\partial}{\partial y}\phi_2 + M_{xy}\left(\frac{\partial}{\partial y}\phi_1 + \frac{\partial}{\partial x}\phi_2\right) + \\ &Q_x\left(\frac{\partial}{\partial x}w_0 + \phi_1\right) + Q_y\left(\frac{\partial}{\partial y}w_0 + \phi_2\right)\Bigg] \\ &\quad -\frac{1}{2}\left(1-\mu^2\nabla^2\right)\left[N_x^b\left(\frac{\partial}{\partial x}w\right)^2 + N_y^b\left(\frac{\partial}{\partial y}w\right)^2\right] - \\ &\left(1-\mu^2\nabla^2\right)\left[\left(K_w w - G_p\nabla^2 w\right)w\right].\end{aligned} \tag{31}$$

3. Analysis of buckling and post-buckling of micro composite cut out plate

The displacement values based on the simply supported rectangular plate can be expressed as [29, 33]

$$w_0(x,y)=w_{mn}\sin\left(\frac{m\pi x}{a}\right)\sin\left(\frac{n\pi y}{b}\right), \tag{32}$$

$$\phi_1(x,y)=\phi_{1mn}\cos\left(\frac{m\pi x}{a}\right)\sin\left(\frac{n\pi y}{b}\right), \tag{33}$$

$$\phi_2(x,y)=\phi_{2mn}\sin\left(\frac{m\pi x}{a}\right)\cos\left(\frac{n\pi y}{b}\right), \tag{34}$$

in which m and n show mode numbers and $\{w_{mn},\phi_{1mn},\phi_{2mn}\}$ are amplitudes. By substituting Eqs. (32-34) to Eq. (31), the following matrix form is extracted

$$(K_L+K_{NL}-FK_G)d=0, \tag{35}$$

where K_L, K_{NL} and K_G represent linear, nonlinear and geometric stiffness matrix, respectively. F is the post bucking load and d is equal to $\{w_{mn},\phi_{1mn},\phi_{2mn}\}^T$.

Eq. (35) can be simplified to linear static buckling formulation of FG-CNTRC micro plate by ignoring nonlinear stiffness matrix such as follow

$$(K_L-F_{cr}K_G)d=0, \tag{36}$$

in which F_{cr} represents the critical buckling load calculated through Rayleigh-Ritz method.

The post-buckling response of the micro plate can be obtained by using Eq. (35) via Rayleigh-Ritz method and Newton-Raphson iterative technique. At the beginning, the iterative scheme starts by solving an eigenvalue problem of Eq. (36) with neglecting the geometric nonlinear matrix to calculate the eigenvalue and corresponding eigenvector such as the first guesses for the buckling load and mode shape. Afterwards, the post-buckling response of plate can be calculated by applying iterative process.

With respect to Figure 1 it is understood that the rectangular plate in this study has central square cut out; therefore, in order to approximate the post-buckling behavior of system, firstly by using domain decomposition method [33-38] the FG-CNTRC micro plate divide to four sections such as Figure 2. After that by using Eq. (31), energy equation of each area is calculated and eventually energy equation of total plate is summation of four areas. Finally, post-buckling response of total plate is extracted by utilizing Eqs. (32-36) through Rayleigh-Ritz method and Newton-Raphson iterative technique.

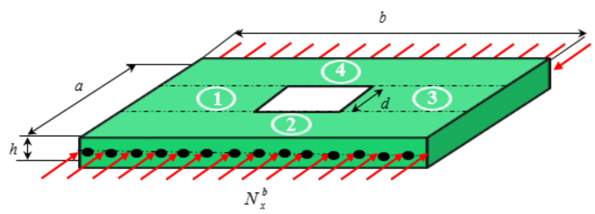

Figure 2. Division of plate into four different areas

2. Results and discussion

Cut out sensitivity on buckling and post-buckling response of micro composite plate reinforced with CNTs and rested in elastic medium subjected to uniaxial load is presented in this dissertation. The variation of buckling and post-buckling of micro composite cut out plate based on some significant parameters such as volume fraction of CNTs, cut out dimension, small scale effect, elastic medium and aspect ratio of plate are studied.

To validate the results of this work with other studies, a comparison among the buckling analysis of this study and Jafari Mehrabadi et al. [4] is considered in Figure 3. In this figure, buckling load in terms of dimension of plate is demonstrated. It is apparent that the present results closely match with those presented by Jafari Mehrabadi et al. [4].

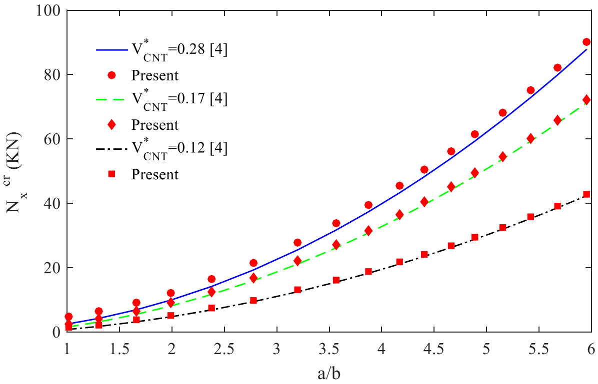

Figure 3. Comparison of buckling load versus dimension of plate for different volume fraction of CNTs

Figure 4 demonstrates a comparison between the results of present article and ref. [39], for a square plate of dimension *a*, with a central square hole of dimension *d*. there is a good agreement for a normalized hole size up to *d/a* = 2.5. For larger size of hole, the difference increases as the size of hole increases. This difference may be attributed to the solving method, because El-Sawy and Nazmy [39] applied FEM but in this study analytical approach used; however, the result of this paper has a good agreement with ref. [39] totally.

Volume fraction of CNTs is one of the important factors of composite plate; thus, variation of buckling load ratio in terms of nonlocal parameter under different volume fraction is showed in Figure 5 whereas the effect of volume fraction on post-buckling versus deflection amplitude according to different volume fractions is examined in Figure 6.

Although by increasing volume fraction the critical buckling load increases but the buckling load ratio decreases, because the variation of local buckling load is more than nonlocal buckling load. In addition, according to Figure 6 it is concluded that increase volume fraction causes more post- buckling load, because volume fraction is a symbol of CNTs volume in composite structure; therefore, increase volume fraction improves mechanical properties of system.

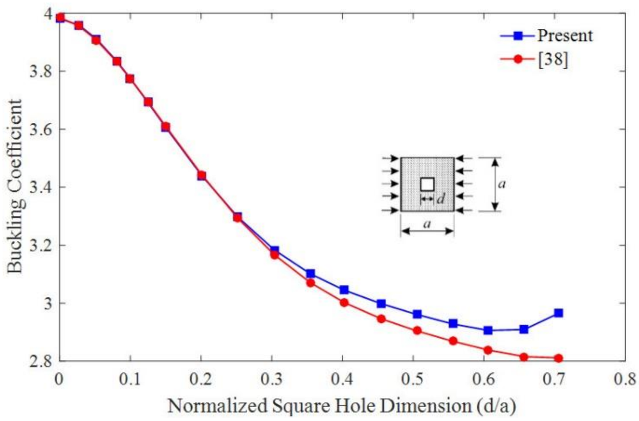

Figure 4. Comparison of buckling coefficient versus normalized square hole dimension

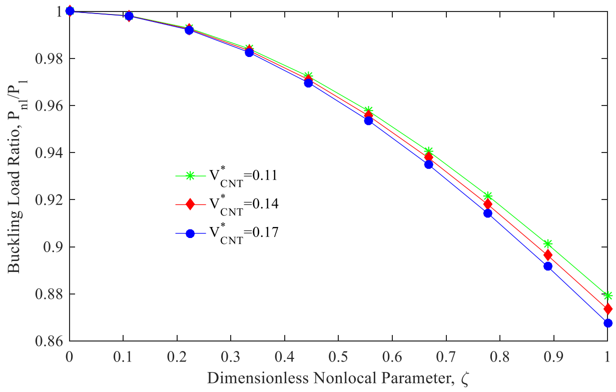

Figure 5. Variation of buckling load ratio in terms of dimensionless nonlocal parameter for different volume fraction

The effect of the elastic medium on buckling response is expressed in this section. Figures 7 and 8 consider the influence of the elastic medium on buckling load based on different magnitude of dimensionless Winkler modulus parameter (K_W) and shear modulus parameter (G_P). It is apparent that Winkler modulus parameter and shear modulus parameter, improve the buckling behavior of micro plate, because considering elastic medium improves the stiffness of system and finally increases buckling load and decreases buckling load ratio.

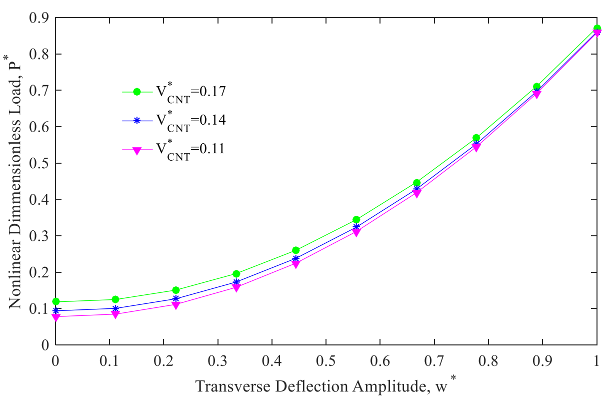

Figure 6. Variation of dimensionless post-buckling load in terms of dimensionless deflection amplitude for different volume fraction

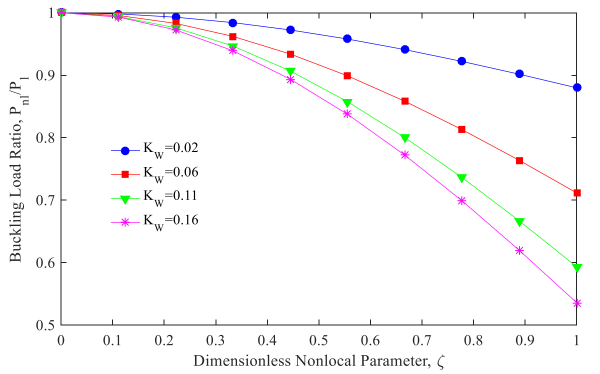

Figure 7. Effect of the Winkler modulus parameter on the buckling load ratio versus dimensionless nonlocal parameter

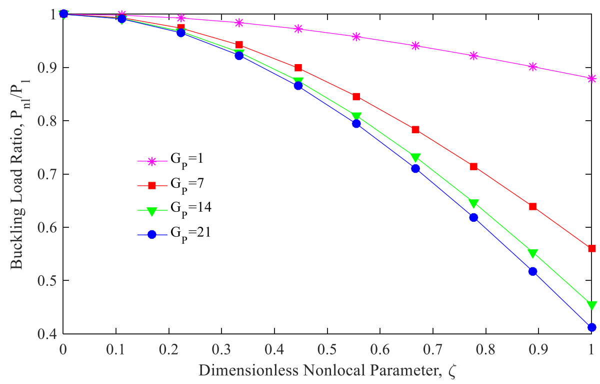

Figure 8. Buckling load ratio versus dimensionless nonlocal parameter for different shear modulus parameter

Moreover, Figures 9 and 10 indicates that variations of the post-buckling load and deflection amplitude are a function of the elastic foundation. It is obvious that considering elastic foundation has positive impact on the post-buckling response of structure. In addition, by analyzing the trend of Figures 9 and 10, the influence of Pasternak foundation is more considerable than Winkler foundation.

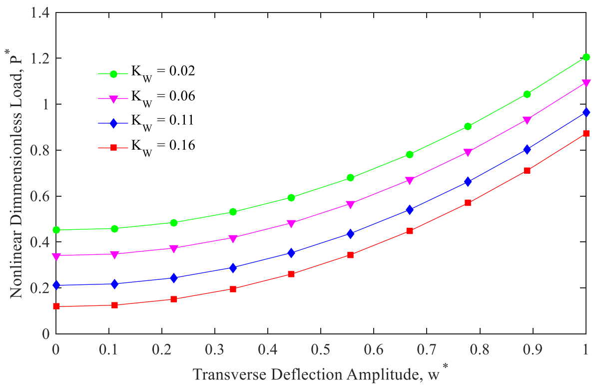

Figure 9. Effect of the Winkler modulus parameter on the dimensionless post-buckling versus dimensionless deflection amplitude

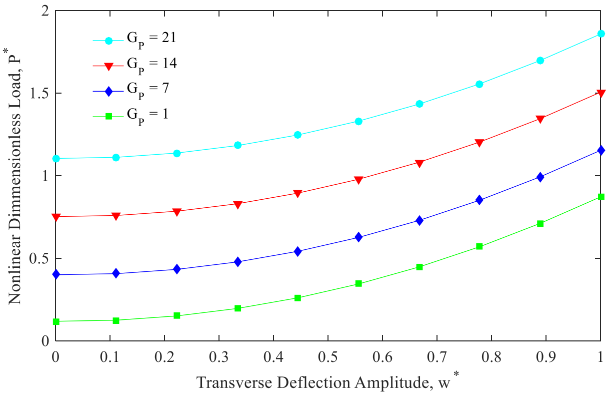

Figure 10. Dimensionless post-buckling load versus dimensionless deflection amplitude for different shear modulus parameter

Figure 11 demonstrates the influence of magnitude of square cut out on the buckling load in terms of small scale effect. It is concluded that opening in plate causes defect in system and reduces the buckling behavior. Moreover, the influence of length of cut out on buckling load ratio is more remarkable for high dimensionless nonlocal parameter. In addition, the variation of dimensionless post-buckling load versus dimensionless deflection in terms of length of square hole is plotted in Figure 12. The figure depicts that by increasing length of square, stiffness of plate reduces; therefore, the post-buckling load decreases subsequently.

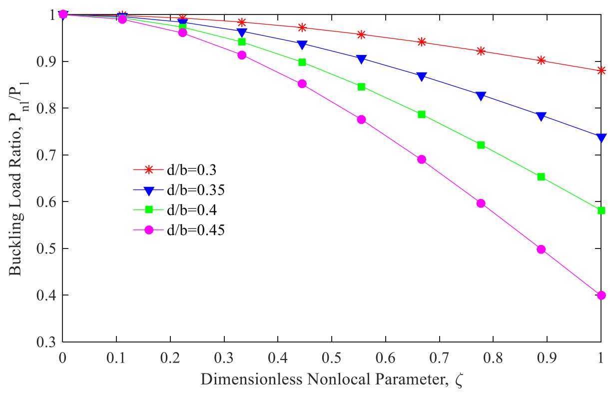

Figure 11. Buckling load ratio versus dimensionless nonlocal parameter for different length of square cut out

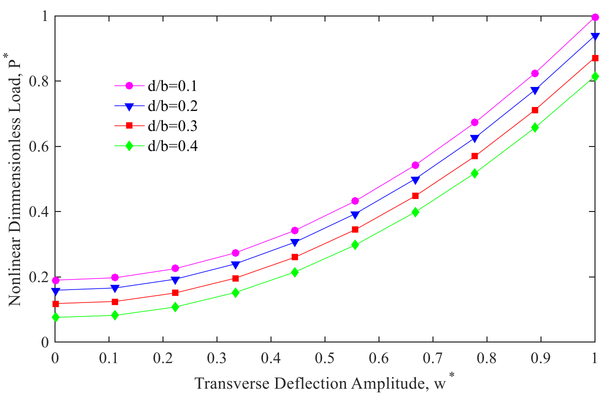

Figure 12. Dimensionless post-buckling load versus dimensionless amplitude of deflection for different length of square cut out

3. Conclusion remarks

In this essay, the effect of central square opening on the buckling and post-buckling response of micro composite plate based on nonlocal elasticity theory and surrounded by elastic medium is considered. By use of Mindlin plate theory and energy method, total energy of system was obtained. Buckling and nonlinear post-buckling of system was analyzed by use of analytical method. The effect of the volume fraction of CNTs, small scale parameter, aspect ratio, square cut out and elastic medium on the buckling and post-buckling behavior of the system were discussed in details. With respect to results, it is concluded that the aspect ratio and length of square cut out have negative effect on buckling and post-buckling response of micro composite plate. Furthermore, existence of CNTs in system causes improvement in the buckling and post-buckling behavior of plate. Meanwhile, considering elastic medium increases the buckling and post-buckling load of system.

References

[1] M. Shishesaz, M. Kharazi, P. Hosseini, M. Hosseini, Buckling Behavior of Composite Plates with a Pre-central Circular Delamination Defect under in-Plane Uniaxial Compression, *Journal of Computational Applied Mechanics*, Vol. 48, No. 1, pp. 111-122, 06/01, 2017. en

[2] A. Zargaripoor, M. Nikkhah bahrami, A wave-based computational method for free vibration and buckling analysis of rectangular Reddy nanoplates, *Journal of Computational Applied Mechanics*, 05/23, 2018. en

[3] H.-S. Shen, C.-L. Zhang, Thermal buckling and postbuckling behavior of functionally graded carbon nanotube-reinforced composite plates, *Materials & Design*, Vol. 31, No. 7, pp. 3403-3411, 2010/08/01/, 2010.

[4] S. Jafari Mehrabadi, B. Sobhani Aragh, V. Khoshkhahesh, A. Taherpour, Mechanical buckling of nanocomposite rectangular plate reinforced by aligned and straight single-walled carbon nanotubes, *Composites Part B: Engineering*, Vol. 43, No. 4, pp. 2031-2040, 2012/06/01/, 2012.

[5] K. M. Liew, Z. X. Lei, J. L. Yu, L. W. Zhang, Postbuckling of carbon nanotube-reinforced functionally graded cylindrical panels under axial compression using a meshless approach, *Computer Methods in Applied Mechanics and Engineering*, Vol. 268, pp. 1-17, 2014/01/01/, 2014.

[6] M. Rafiee, X. Q. He, S. Mareishi, K. M. Liew, Nonlinear Response of Piezoelectric Nanocomposite Plates: Large Deflection, Post-Buckling and Large Amplitude Vibration, *International Journal of Applied Mechanics*, Vol. 07, No. 05, pp. 1550074, 2015/10/01, 2015.

[7] M. Jamali, T. Shojaee, R. Kolahchi, B. Mohammadi, Buckling analysis of nanocomposite cut out plate using domain decomposition method and orthogonal polynomials, *Steel and Composite Structures*, Vol. 22, pp. 691-712, 2016.

[8] M. Z. Nejad, A. Hadi, A. Rastgoo, Buckling analysis of arbitrary two-directional functionally graded Euler–Bernoulli nano-beams based on nonlocal elasticity theory, *International Journal of Engineering Science*, Vol. 103, pp. 1-10, 2016.

[9] M. Z. Nejad, A. Hadi, Non-local analysis of free vibration of bi-directional functionally graded Euler–Bernoulli nano-beams, *International Journal of Engineering Science*, Vol. 105, pp. 1-11, 2016.

[10] R. Kolahchi, A. Cheraghbak, Agglomeration effects on the dynamic buckling of viscoelastic microplates reinforced with SWCNTs using Bolotin method, *Nonlinear Dynamics*, Vol. 90, No. 1, pp. 479-492, 2017/10/01, 2017.

[11] M. Z. Nejad, A. Hadi, A. Farajpour, Consistent couple-stress theory for free vibration analysis of Euler-Bernoulli nano-beams made of arbitrary bi-directional functionally graded materials, *Structural Engineering & Mechanics*, Vol. 63(2), pp. 161-169, 07/25, 2017. En

[12] A. Hadi, M. Z. Nejad, A. Rastgoo, M. Hosseini, Buckling analysis of FGM Euler-Bernoulli nano-beams with 3D-varying properties based on consistent couple-stress theory, *Steel and Composite Structures*, Vol. 26(6), 03/25, 2018. En

[13] M. Z. Nejad, A. Hadi, A. Omidvari, A. Rastgoo, Bending analysis of bi-directional functionally graded Euler-Bernoulli nano-beams using integral form of Eringen's non-local elasticity theory, *Structural Engineering and Mechanics,* Vol. 67, No. 4, pp. 417-425, 2018.

[14] A. Farajpour, A. Arab Solghar, A. Shahidi, Postbuckling analysis of multi-layered graphene sheets under non-uniform biaxial compression, *Physica E: Low-dimensional Systems and Nanostructures,* Vol. 47, pp. 197-206, 2013/01/01/, 2013.

[15] K. F. Wang, B. L. Wang, Effect of surface energy on the non-linear postbuckling behavior of nanoplates, *International Journal of Non-Linear Mechanics,* Vol. 55, pp. 19-24, 2013/10/01/, 2013.

[16] A. Naderi, A. R. Saidi, Nonlocal postbuckling analysis of graphene sheets in a nonlinear polymer medium, *International Journal of Engineering Science,* Vol. 81, pp. 49-65, 2014/08/01/, 2014.

[17] M. Akbarzadeh Khorshidi, M. Shariati, S. A. Emam, Postbuckling of functionally graded nanobeams based on modified couple stress theory under general beam theory, *International Journal of Mechanical Sciences,* Vol. 110, pp. 160-169, 2016/05/01/, 2016.

[18] S. Sahmani, M. M. Aghdam, M. Bahrami, Size-dependent axial buckling and postbuckling characteristics of cylindrical nanoshells in different temperatures, *International Journal of Mechanical Sciences,* Vol. 107, pp. 170-179, 2016/03/01/, 2016.

[19] H. Wu, S. Kitipornchai, J. Yang, Thermal buckling and postbuckling of functionally graded graphene nanocomposite plates, *Materials & Design,* Vol. 132, pp. 430-441, 2017/10/15/, 2017.

[20] S. Thai, H.-T. Thai, T. P. Vo, S. Lee, Postbuckling analysis of functionally graded nanoplates based on nonlocal theory and isogeometric analysis, *Composite Structures,* Vol. 201, pp. 13-20, 2018/10/01/, 2018.

[21] Y. M. Ghugal, A. S. Sayyad, A Static Flexure of Thick Isotropic Plates Using Trigonometric Shear Deformation Theory, *Journal of Solid Mechanics,* Vol. 2, No. 1, pp. 79-90, 03/30, 2010. en

[22] A. Ghorbanpour Arani, R. Kolahchi, H. Vossough, Buckling analysis and smart control of SLGS using elastically coupled PVDF nanoplate based on the nonlocal Mindlin plate theory, *Physica B: Condensed Matter,* Vol. 407, No. 22, pp. 4458-4465, 2012/11/15/, 2012.

[23] M. Bedroud, R. Nazemnezhad, S. Hosseini-Hashemi, M. Valixani, Buckling of FG circular/annular Mindlin nanoplates with an internal ring support using nonlocal elasticity, *Applied Mathematical Modelling,* Vol. 40, No. 4, pp. 3185-3210, 2016/02/15/, 2016.

[24] C. Liu, L.-L. Ke, J. Yang, S. Kitipornchai, Y.-S. Wang, Buckling and post-buckling analyses of size-dependent piezoelectric nanoplates, *Theoretical and Applied Mechanics Letters,* Vol. 6, No. 6, pp. 253-267, 2016/11/01/, 2016.

[25] A. Soleimani, M. H. Naei, M. M. Mashhadi, Nonlocal postbuckling analysis of graphene sheets with initial imperfection based on first order shear deformation theory, *Results in Physics,* Vol. 7, pp. 1299-1307, 2017/01/01/, 2017.

[26] A. Daneshmehr, A. Rajabpoor, A. Hadi, Size dependent free vibration analysis of nanoplates made of functionally graded materials based on nonlocal elasticity theory with high order theories, *International Journal of Engineering Science,* Vol. 95, pp. 23-35, 2015.

[27] A. Ghorbanpour Arani, M. Jamali, M. Mosayyebi, R. Kolahchi, Wave propagation in FG-CNT-reinforced piezoelectric composite micro plates using viscoelastic quasi-3D sinusoidal shear deformation theory, *Composites Part B: Engineering,* Vol. 95, pp. 209-224, 2016/06/15/, 2016.

[28] H. Akhavan, S. Hosseini Hashemi, H. R. Damavandi Taher, A. Alibeigloo, S. Vahabi, Exact solutions for rectangular Mindlin plates under in-plane loads resting on Pasternak elastic foundation. Part I: Buckling analysis, *Computational Materials Science,* Vol. 44, No. 3, pp. 968-978, 2009/01/01/, 2009.

[29] S. H. Hashemi, A. T. Samaei, Buckling analysis of micro/nanoscale plates via nonlocal elasticity theory, *Physica E: Low-dimensional Systems and Nanostructures,* Vol. 43, No. 7, pp. 1400-1404, 2011/05/01/, 2011.

[30] A. T. Samaei, S. Abbasion, M. M. Mirsayar, Buckling analysis of a single-layer graphene sheet embedded in an elastic medium based on nonlocal Mindlin plate theory, *Mechanics Research Communications,* Vol. 38, No. 7, pp. 481-485, 2011/10/01/, 2011.

[31] A. C. Eringen, 2002, *Nonlocal Continuum Field Theories*,

[32] A. Ghorbanpour Arani, M. Jamali, A. H. Ghorbanpour-Arani, R. Kolahchi, M. Mosayyebi, Electro-magneto wave propagation analysis of viscoelastic sandwich nanoplates considering surface effects, *Proceedings of the Institution of Mechanical Engineers, Part C: Journal of Mechanical Engineering Science,* Vol. 231, No. 2, pp. 387-403, 2017/01/01, 2016.

[33] R. Ali, S. J. Atwal, Prediction of natural frequencies of vibration of rectangular plates with rectangular cutouts, *Computers & Structures,* Vol. 12, No. 6, pp. 819-823, 1980/12/01/, 1980.

[34] K. M. Liew, S. Kitipornchai, A. Y. T. Leung, C. W. Lim, Analysis of the free vibration of rectangular plates with central cut-outs using the discrete Ritz method, *International Journal of Mechanical Sciences,* Vol. 45, No. 5, pp. 941-959, 2003/05/01/, 2003.

[35] Z. Pan, Y. Cheng, J. Liu, A semi-analytical analysis of the elastic buckling of cracked thin plates under axial compression using actual non-uniform stress distribution, *Thin-Walled Structures,* Vol. 73, pp. 229-241, 2013/12/01/, 2013.

[36] K. Y. Lam, K. C. Hung, S. T. Chow, Vibration analysis of plates with cutouts by the modified Rayleigh-Ritz method, *Applied Acoustics,* Vol. 28, No. 1, pp. 49-60, 1989/01/01/, 1989.

[37] K. M. Liew, K. C. Hung, M. K. Lim, Method of domain decomposition in vibrations of mixed edge anisotropic plates, *International Journal of Solids and Structures,* Vol. 30, No. 23, pp. 3281-3301, 1993/01/01/, 1993.

[38] K. M. Liew, T. Y. Ng, S. Kitipornchai, A semi-analytical solution for vibration of rectangular plates with abrupt thickness variation, *International Journal of Solids and Structures,* Vol. 38, No. 28, pp. 4937-4954, 2001/07/01/, 2001.

[39] K. M. El-Sawy, A. S. Nazmy, Effect of aspect ratio on the elastic buckling of uniaxially loaded plates with eccentric holes, *Thin-Walled Structures,* Vol. 39, No. 12, pp. 983-998, 2001/12/01/, 2001.